Continuous time random walk model for standard map dynamics

R. Balescu*
Association Euratom–Etat Belge pour la Fusion, Physique Statistique et Plasmas, CP 231, Université Libre de Bruxelles, 1050 Bruxelles, Belgium
(Received 21 August 1996)

In standard map dynamics, the time series x_t are analyzed for chaotic orbits bounded by Kolmogorov-Arnold-Moser barriers, for subcritical values of the stochasticity parameter. They can be described as a succession of rather regular oscillations of bounded amplitude in basins located near island chains, and of jumps between basins, at ''random'' times. This motion can be adequately modeled by a continuous time random walk, using values of the parameters taken from the numerical data. The resulting theory describes a subdiffusive motion, for which the mean square displacement tends towards a saturation value. [S1063-651X(97)06003-0]

PACS number(s): 05.40.+j, 05.45.+b, 05.60.+w

I. INTRODUCTION

The problem of *anomalous transport* can be defined quite generally, but vaguely, as transport (of matter or energy) in a medium that is *strongly disordered*. The cause of this disorder may be structural (such as in a porous material), or may be due to the presence of strong and irregular collective fluctuations (as in a turbulent fluid or plasma). The name ''disordered'' rightly suggests that such systems are too complex for a detailed deterministic study: we are compelled to resort to *statistical or probabilistic methods* for the study of such problems.

When the ''degree of disorder'' is very large, the system considered appears almost homogeneous on a macroscopic scale. This makes the statistical treatment very efficient. In an extremely disordered system, when a characteristic ''stochasticity parameter'' is very large, the transport processes behave almost classically, although the transport coefficients depend on the stochasticity parameter (hence on the degree of disorder), and the driving mechanism is not collisional. Such processes are called *diffusive, but anomalous.*

Real disordered systems are not ''ideally disordered'' in the sense discussed above. Most often, there exist orderly structures immersed irregularly in a ''chaotic sea.'' Such *islands* have a deep influence on the transport processes. The latter are no longer classical; these phenomena will be called *''strange diffusion processes''* [1]. They may result in transport that is slower than the expected diffusive one (*subdiffusive regime*), or faster than the diffusive one (*superdiffusive regime*).

Strange transport is a very important problem, having many practical applications. It is also an extremely difficult problem, because it occurs in systems that are neither ideally ordered, nor ideally disordered. There are extremely few exact analytical results available. In the majority of cases, one has to resort to numerical simulations, which may suggest approximate mathematical models, which in turn, may possibly be treated analytically (or semianalytically).

In principle, the study of the evolution of a material system should start from the equations of motion. It is, however, known that these are, generically, nonintegrable. They must therefore be solved numerically. But even this is usually impossible, because a minimal degree of precision requires constraints that are not realizable even with the most powerful modern computers. A widely used method consists then of replacing the differential equations of motion by a *map*, i.e., replacing the continuous time description by a discrete one.

In the present work we shall consider the famous *standard map* introduced by Chirikov [2–4]. This map has been used for modeling many physical phenomena. A problem that reduces locally to the standard map is the diffusion of magnetic lines in a tokamak or a stellarator [5,6] (although the model is not quite faithful [7]).

In the limit of very large stochasticity parameter K the standard map has been extensively studied. In a pioneering work, Rechester and White [8] showed that the behavior of test particles obeying standard map dynamics becomes *diffusive.* They calculated the corresponding anomalous diffusion coefficient, which was refined in subsequent works [9–11] (see also [3]). It was also shown that in the same domain of large stochasticity parameter, the behavior may become ''strange,'' i.e. *superdiffusive* for certain values *of K* [12–15]. The latter behavior, due to the presence of ''accelerator modes,'' is very interesting, but not generic: it is a specific feature of the standard model.

The dynamics of chaotic orbits in the standard map in a domain of moderately large, subcritical values of the stochasticity parameter has been much less studied. It is, however, a very important regime in practical applications. For instance, in the tokamak problem, we must be sure that the magnetic field lines (and, hopefully, the plasma) remain confined in the toroidal chamber. In this regime the particles can only be dispersed in a limited region of space, because of the presence of impermeable KAM barriers. It appears that in this case the process is *subdiffusive.* As will be seen in Sec. II, the motion of the particles is strongly suggesting a *continuous time random walk* (CTRW) [16–19]. This analogy was previously noted by White *et al.* [20]. Their model and its implementation are, however, very different from ours: it will be briefly discussed in Sec. II.

*Electronic address: rbalescu@resulb.ulb.ac.be

Our approach is semianalytical. An analysis of a long time series (Sec. III) reveals a number of (statistically) simple features of the standard map dynamics. The latter can be described as a rather regular motion of the particle within a ''basin,'' followed by a jump to another basin, where the motion is again rather regular, etc. Based on this picture, we simplify the present problem of deterministic chaos by considering that its only random features are the transition probabilities between basins and the duration of the sojourn in a given basin. These are precisely the ingredients necessary for the definition of a CTRW. The latter is defined and solved analytically in Sec. III. In a simple case, the problem can be made quite explicit, by using numbers determined from the numerical calculations (Sec. IV). In Sec. V the explicit solution of this simple case is obtained and analyzed: the running diffusion coefficient tells us how the final asymptotic state is reached.

II. TIME SERIES IN THE STANDARD MAP

We consider the well-known dynamical system known as Chirikov's standard map [2–4], defined by the following equations describing the instantaneous values x_t, θ_t of the two coordinates of a ''particle'' (θ being an angle measured in radians divided by 2π) at the regular times t (where t is an integer):

$$x_{t+1} = x_t - \frac{K}{2\pi}\sin 2\pi\theta_t,$$

$$\theta_{t+1} = \theta_t + x_{t+1} (\mathrm{mod}\, 1). \tag{1}$$

The real number $K \geqslant 0$ is the *stochasticity parameter*. It is well known that, for $K > 0$, a variety of types of orbits are possible: *cycles* (periodic orbits), *island chains* (encircling the cycles), *KAM barriers*, and *chaotic orbits*. For small K, the latter are limited to finite regions of phase space, bounded by island chains and KAM barriers. As K increases, the barriers are progressively destroyed by the appearance of ''holes'' which transform them into permeable *cantori*. There exists a critical value, $K = K_c$, when the last (''golden'') KAM barrier is destroyed, and the chaotic orbits can reach arbitrary values of x [21]; the value of the critical K is $K_c = 0.971\,635\ldots$.

We are interested in the dynamics of these systems for $K < K_c$. The regime under discussion corresponds to a situation of *partially chaotic dynamics*. A typical chaotic orbit is shown in Fig. 1.

The golden KAM is an absolute barrier in this case. Moreover, depending on the value of K, there may be additional barriers defining regions in phase space whose boundaries cannot be crossed by any chaotic orbit. In Fig. 1 there are two clearly visible regions differing by the density of the phase points: the boundary between them is a *cantorus*. The orbit starting in the upper part had to wait for a relatively long time before finding its way through a hole in the latter. In the situation represented in Fig. 1 there appear clearly *four ''main'' island chains* that are clearly identifiable by the ''large'' size of the islands. Clearly, the distinction between ''large'' and ''small'' islands is arbitrary. The forthcoming treatment does not depend on where the limit is set, provided

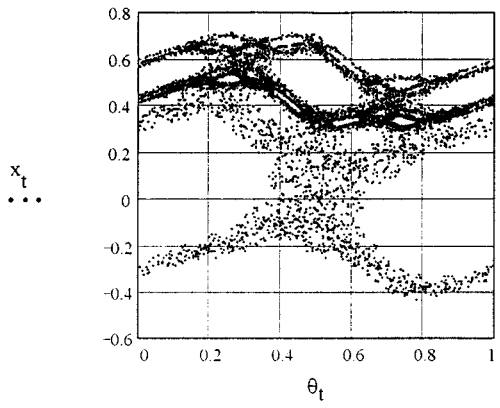

FIG. 1. A chaotic orbit for $K = 1.15$, represented in the phase space (x_t, θ_t) (7500 iterations, starting from $x_0 = 0.4, \theta_0 = 0.75$).

the number of ''large'' islands is specified at the beginning. There are also, of course, secondary islands around each ''large'' island: these will be, by convention, included into the main island chain (the term ''included'' will be defined more precisely below).

Our main interest lies in the chaotic orbits. We shall study the way in which a set of particles starting with an arbitrary initial distribution in a certain region, bounded by two successive KAM barriers, is eventually dispersed and fills the entire phase space region included between the limiting KAM barriers and the island boundaries (as in Fig. 1). Alternatively, assuming the validity of (some kind of) an ergodic property, one may follow a single chaotic trajectory for a long time (i.e., by calculating many iterations of the standard map). Keeping in mind the application to the problem of magnetic field line diffusion in a tokamak, the main interest lies in a reduced problem, viz., the *''diffusion'' in the radial direction*, which corresponds to the x direction in the standard map. The complete solution of this problem would involve the determination of the *density profile* $n(x;t)$; this quantity is, however, not easily accessible, either analytically or numerically. A good (and usual) indicator of the dispersion is the *mean square deviation* (MSD): $\langle \delta x^2(t) \rangle$. This is easily measured numerically; our purpose here will be to devise an analytical model for its determination.

It is pretty clear *a priori* that *the evolution process in the case $K < K_c$ cannot be diffusive.* Indeed, because of the presence of the KAM barriers, the MSD will necessarily *saturate* asymptotically, as $t \to \infty$. The final value will be essentially the square of the width of the region. This is in contrast with a diffusive process, in which the MSD exhibits an unbounded growth, proportional to time. The effective diffusion coefficient (defined more precisely below) is thus necessarily zero:

$$D \equiv \frac{1}{2}\lim_{t\to\infty}\frac{d}{dt}\langle \delta x^2(t) \rangle = 0. \tag{2}$$

We are thus in presence of a strongly *subdiffusive behavior*.

The interesting problem is to study the dynamics of the approach to the saturated steady state. A useful tool for this purpose is the graph of the x coordinate as a function of

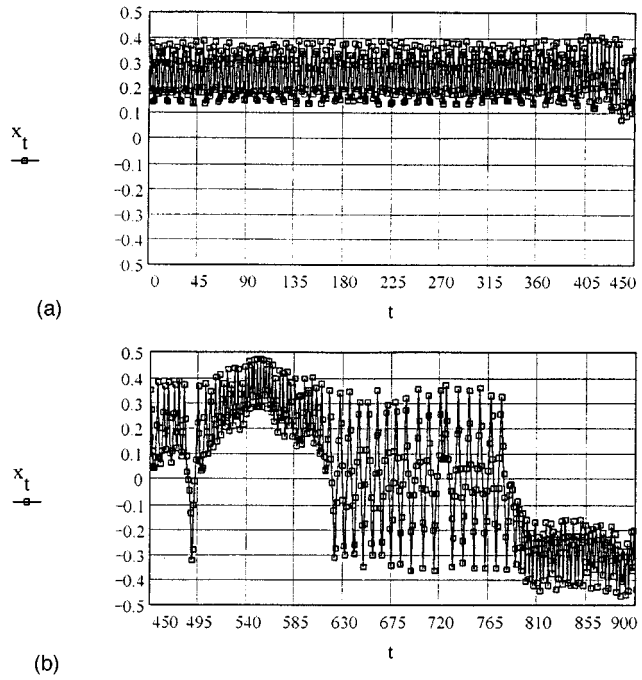

FIG. 2. (a) Time series for x_t of a chaotic orbit in the standard map. $K=1.2$ ($x_0=0.18$, $\theta_0=0.51$), for $0\leqslant t\leqslant 450$. (b) Same orbit as in (a), for $450\leqslant t\leqslant 900$.

(discrete) time t: it provides us with a very different view of the evolution process. (One may, of course, also plot the angle θ as a function of time; for the reasons explained above, this information is less interesting for the applications.) The complete graph of x_t vs t for a long trajectory requires, of course, a *very long* sheet of paper. The analysis can be done, however, by using successive short sections of this graph, as in Figs. 2(a) and 2(b).

This type of evolution is very peculiar. We see a first period [Fig. 2(a)] roughly between $t=0$ and $t=450$ where the particle oscillates fairly regularly between two limits ($0.1<x<0.4$); at $t\approx 480$ there is a sudden jump down to $x\approx -0.35$; between $t\approx 540$ and 560 there is an oscillation between 0.28 and 0.48; between $t\approx 600$ and 780 there is an oscillation between 0.38 and -0.38, etc. The situation is adequately described in terms of a set of basins. *A basin* is defined as a region, bounded above and below in x, in which a particle remains trapped for at least two oscillations in x between the bounds, before it jumps to another basin. Different basins may overlap in x. A particle moving on a chaotic orbit starts at time zero in a basin, and remains confined in it for some time; at some instant, it jumps suddenly to another basin and starts oscillating for some time in the latter, after which another sudden jump brings it into another basin, etc. The duration of the sojourn in a basin is extremely variable: it may be as short as 10 iterations or as long as 10 000. The times at which the jumps occur do not seem to exhibit any regularity. When looking at a long trajectory, the effect is particularly striking. The basins are clearly located in the (external) neighborhood of the island chains. The peculiar type of motion is thus a consequence of the *sticking property* of the island chains and of the cantori [22–26]. Our results show that the influence of a given island can extend far in phase space (for $K<K_c$), to the point that the whole available phase space for a chaotic orbit can be subdivided into basins connected to the islands. On the other hand (as will be seen below), a basin is not defined merely as the whole neighborhood of an island.

This type of evolution immediately suggests the picture of a *continuous time random walk* (CTRW) [16–19]. The idea of representing the evolution in a standard map by a random walk was already used in a work by White *et al.* [20]: they use the suggestive description of the motion as ''*step-pause-step-pause-* . . . .'' Their model is, however, different and the results cannot be compared to ours. A typical application of our model is the ''diffusion'' of magnetic field lines in a tokamak. The ''particles'' represented by the coordinates (x_t,θ_t) are the intercepts of a given magnetic field line with a plane perpendicular to the magnetic axis. The work of White *et al.* aims at modeling the motion of physical charged particles moving in a stochastic magnetic field (represented by a standard map) and undergoing collisions. The latter are represented by an additional noise superimposed on the standard map. This additional stochasticity combined with the deterministic chaos changes rather radically the nature of the problem.

The motion of the particles as illustrated in Figs. 2(a) and 2(b) also suggests a possible analogy with the phenomenon of *intermittence* as observed in turbulent flows. The underlying physics in the latter problem is, however, very different and we cannot tell at present whether the analogy is more than superficial.

In the present work, the motion is idealized as follows. At time $t=0$, a large number of particles is distributed in the phase space. The particles can be subdivided into two classes. The ''*jailed particles*'' are those whose initial position lies inside an island chain. For all subsequent times they perform a strictly periodic motion, remaining inside the island chain where they started. The particles in the complementary set, whose initial coordinates are located outside the island chains, are called *active particles:* for $t\to\infty$ they tend to fill in all the space between the islands, bounded by two successive KAM barriers. These will be the main object of interest in the forthcoming work. For brevity we agree to call simply ''particles'' the active particles, unless explicitly stated to the contrary.

We consider the evolution in time of the coordinate x_t. Any given (active) particle remains in a basin for some time, then jumps abruptly to another basin, etc. We shall not be interested in the details of the motion within a given basin. Rather, we assume that the process, starting at a given initial value, is described *statistically:* the motion is then completely defined by the specification of three features: *the location of the relevant basins in phase space, the probability of a sojourn of length t in a given basin,* and *the transition probability between two basins.* This picture is, of course, a serious simplification of the exact motion. It amounts to declaring that the whole ''randomness'' associated with the deterministic chaos of the standard map is concentrated in the ''statistics of the jumps between basins.'' The shape of the time series such as those shown in Fig. 2 justifies this statement.

III. THE STANDARD MAP CTRW

The first point mentioned above, i.e., the location of the *relevant* basins, depends on the value of the stochasticity

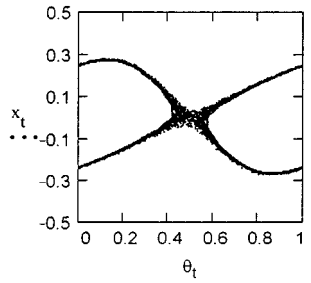

FIG. 3. A chaotic orbit for $K=0.7(<K_c)$, represented in phase space $(x_0=0.25, \theta_0=0)$.

parameter and on the initial condition. We develop here a general analytical formalism which is illustrated by a very simple particular case. In this example, the stochasticity parameter is chosen to be well below the critical threshold, but not too small (in order to produce sufficiently large chaotic regions); specifically, we choose $K=0.7$. The portion of phase space under consideration is taken as the region bounded by the main island around (0,0) and the nearest undestroyed KAM barriers above $(x>0)$ and below $(x<0)$ this island; a typical chaotic orbit is shown in Fig. 3.

One can recognize near the boundary of the main island a number of small secondary islands. In the time series, they do not, however, appear as a distinct entity (with a well-defined attached basin). They are therefore not counted separately, but rather are supposed to belong to the chaotic region.

We now consider a time series, as in Fig. 2. It clearly appears that the x coordinate sojourns successively in three regions: these are the *relevant basins* for $K=0.7$ and for the present configuration (Fig. 3) of the phase space. The three basins appear very clearly in the section of a chaotic orbit shown in Fig. 4. (Specifically, this figure represents the section $2700<t<3700$ of the orbit starting at $x_0=0.2$, $\theta_0=0.88$.)

This situation clarifies our previous remark: the basins are not necessarily related, one to one, to the island chains. In the present case there is *a single island* [centered on (0,0)], but there are *three basins.* The latter correspond to the whole island, to the upper half of the island, and to its lower half, respectively. Thus, the basins do not represent a geometrical feature of the phase space, but rather a *dynamical property*, related to the way in which the orbit is covered in the course of time.

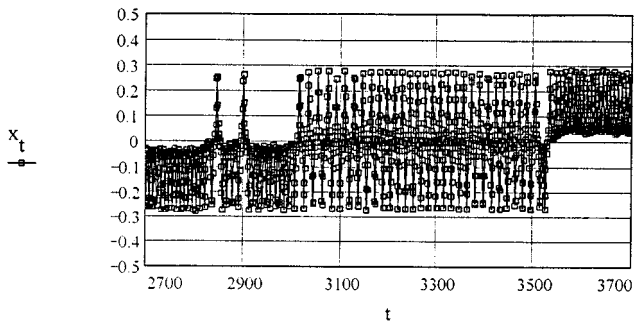

FIG. 4. Section of time series for x_t of a chaotic orbit $(x_0=0.2,\ \theta_0=0.88)$.

Having identified the relevant basins, we construct a CTRW model describing approximately this dynamics. (A similar, but not identical problem is treated in the monograph [18] under the name of ''multistate CTRW''.) We recall that we are only considering here the distribution of active particles among the relevant basins. The latter will be labeled by a Latin subscript, e.g., $m=1,2,\ldots,M$, where M is the number of relevant basins in the problem. In our example, $M=3$; the labels are chosen (conventionally) as follows: $m=1$, whole island basin; $m=2$, upper half island basin; $m=3$, lower half island basin.

The random walk (i.e., the ''dynamics'') is completely determined by the quantities $n_m(t)$: the *probability of finding a particle in basin m at time t*. These quantities can be considered as the components of an M-component vector $\mathbf{n}(t)$. In our example,

$$\mathbf{n}(t)=[n_1(t),n_2(t),n_3(t)]. \tag{3}$$

We also use the abbreviated notation $\mathbf{n}^0\equiv\mathbf{n}(0)$ [or $n_m^0\equiv n_m(0)$ for the components] for the initial condition. Next, we define the *waiting time distribution* (WTD). In the classical CTRW problem [17–19], there is a single function $\psi(t)$ characterizing completely this quantity. Here, the waiting time distribution can be different in the various basins. We thus define $p_m(t)$ as the *probability that a particle, entering the basin m, makes a transition to another basin after a time t*. It appears that these quantities must be considered as components of a diagonal $M\times M$ matrix, $\mathsf{P}(t)$. In our example this matrix is

$$\mathsf{P}(t)=\begin{pmatrix} p_1(t) & 0 & 0 \\ 0 & p_2(t) & 0 \\ 0 & 0 & p_3(t) \end{pmatrix}. \tag{4}$$

Thus, in general, the matrix elements of $\mathsf{P}(t)$ are

$$\langle m|\mathsf{P}(t)|n\rangle=p_m(t)\,\delta_{mn}. \tag{5}$$

The last ingredient necessary for the definition of the CTRW is the *transition probability f_{mn} from basin n to basin m :* the set of these quantities defines a matrix F:

$$\langle m|\mathsf{F}|n\rangle=f_{mn}. \tag{6}$$

By definition, the diagonal elements are identically zero. Thus, in our example we have

$$\mathsf{F}=\begin{pmatrix} 0 & f_{12} & f_{13} \\ f_{21} & 0 & f_{23} \\ f_{31} & f_{32} & 0 \end{pmatrix}. \tag{7}$$

We now start the solution of the problem. We note that the probability that at least one jump has occurred out of the basin m during the interval $[0,t]$ is the integral of $p_m(\tau)$ from 0 to t; hence, the probability that a particle, entering basin m at time zero, is still there at time t is

$$r_m(t)=1-\int_0^t d\tau\, p_m(\tau), \tag{8}$$

or, performing a Laplace transformation,

$$\hat{r}_m(s)=\frac{1}{s}[1-\hat{p}_m(s)].$$

These quantities are grouped into a diagonal matrix [because of Eq. (5)]:

$$\hat{\mathsf{R}}(s)=\frac{1}{s}[\mathsf{I}-\hat{\mathsf{P}}(s)]. \tag{9}$$

Let now $q_m(t)$ be the probability that a particle arrives in basin m *just after a jump.* Then, the probability $n_m(t)$ is obtained by considering the probability $q_m(\tau)$ of landing in basin m just at time τ, multiplied by the probability that it is still in m at time t, and summed over all intermediate times τ:

$$n_m(t)=\int_0^t d\tau\, r_m(t-\tau)q_m(\tau),$$

or, in matrix notation and in Laplace representation:

$$\hat{\mathbf{n}}(s)=\frac{1}{s}[\mathsf{I}-\hat{\mathsf{P}}(s)]\cdot\hat{\mathbf{q}}(s). \tag{10}$$

In order to calculate the quantity $q_m(t)$ we consider successively the cases where the particle that started in basin k at $t=0$ lands in m at time t in j steps. For $j=1$, the particle remains in basin k for a time t and makes a jump to m at that time; thus

$$q_m^{(1)}(t)=\sum_k f_{mk}p_k(t)n_k^0.$$

For $j=2$, the particle waits in basin k from $t=0$ to τ, jumps to basin l, then waits there till t, when it jumps to m:

$$\begin{aligned}q_m^{(2)}(t)&=\sum_{k,l}\int_0^t d\tau f_{ml}p_l(t-\tau)f_{lk}p_k(\tau)n_k^0\\&=\sum_l\int_0^t d\tau f_{ml}p_l(t-\tau)q_l^{(1)}(\tau).\end{aligned}$$

This argument is easily generalized for arbitrary j, yielding a recurrence relation:

$$q_m^{(j)}(t)=\sum_k\int_0^t d\tau f_{mk}p_k(t-\tau)q_k^{(j-1)}(\tau), \tag{11}$$

which must be solved with the condition

$$q_k^{(0)}(\tau)=n_k^0\delta(\tau). \tag{12}$$

It is easily checked, using the forms (4) and (7) that Eq. (11) is written in matrix form as follows:

$$\mathbf{q}^{(j)}(t)=\int_0^t d\tau\,\mathsf{F}\cdot\mathsf{P}(t-\tau)\cdot\mathbf{q}^{(j-1)}(\tau). \tag{13}$$

[At this point it clearly appears that the remarkable factorization appearing in Eq. (13) is ensured by our defining the quantities $p_m(t)$ as components of a *diagonal matrix*, rather than a vector.] In the Laplace representation, Eq. (13) becomes an algebraic equation:

$$\hat{\mathbf{q}}^{(j)}(s)=\mathsf{F}\cdot\hat{P}(s)\cdot\hat{\mathbf{q}}^{(j-1)}(s),$$

which is easily solved, yielding

$$\hat{\mathbf{q}}^{(j)}(s)=[\mathsf{F}\cdot\hat{\mathsf{P}}(s)]^j\cdot\mathbf{n}^0.$$

We now sum this result over j in order to obtain the total probability vector $\hat{\mathbf{q}}(s)$:

$$\hat{\mathbf{q}}(s)=[\mathsf{I}-\mathsf{F}\cdot\hat{\mathsf{P}}(s)]^{-1}\cdot\mathbf{n}^0. \tag{14}$$

Finally, we substitute this result in Eq. (10) and obtain

$$\hat{\mathbf{n}}(s)=\frac{1}{s}[\mathsf{I}-\hat{\mathsf{P}}(s)]\cdot[\mathsf{I}-\mathsf{F}\cdot\hat{\mathsf{P}}(s)]^{-1}\cdot\mathbf{n}^0. \tag{15}$$

This equation provides us with the complete solution of the initial value problem for our CTRW. It is very similar to the well-known *Montroll-Weiss equation* [16–19] adapted to our problem. It expresses the Laplace transform of the probability of the distribution of particles among basins, in terms of the initial condition $\mathbf{n}^0$ and of the input information expressed by the waiting time distribution $\hat{\mathsf{P}}(s)$ and the transition probabilities F. For our simple example, a straightforward calculation yields the following form for solution (15) in the Laplace representation:

$$\begin{aligned}\hat{n}_1(s)&=\frac{1-\hat{p}_1}{s\hat{\Delta}}[(4-\hat{p}_2\hat{p}_3)n_1^0+(2+\hat{p}_3)\hat{p}_2n_2^0\\&\quad+(2+\hat{p}_2)\hat{p}_3n_3^0],\\\hat{n}_2(s)&=\frac{1-\hat{p}_2}{s\hat{\Delta}}[(2+\hat{p}_3)\hat{p}_1n_1^0+(4-\hat{p}_1\hat{p}_3)n_2^0\\&\quad+(2+\hat{p}_1)\hat{p}_3n_3^0],\\\hat{n}_3(s)&=\frac{1-\hat{p}_3}{s\hat{\Delta}}[(2+\hat{p}_2)\hat{p}_1n_1^0+(2+\hat{p}_1)\hat{p}_2n_2^0\\&\quad+(4-\hat{p}_1\hat{p}_2)n_3^0],\end{aligned} \tag{16}$$

with

$$\hat{\Delta}=4-\hat{p}_1\hat{p}_2-\hat{p}_1\hat{p}_3-\hat{p}_2\hat{p}_3-\hat{p}_1\hat{p}_2\hat{p}_3 \tag{17}$$

(all symbols with a caret denote functions of s).

An equation of evolution for $\hat{\mathbf{n}}(s)$ is easily derived from Eq. (15) (see [17–19]):

$$s\hat{\mathbf{n}}(s)-\mathbf{n}^0=-(\mathsf{I}-\mathsf{F})\cdot\hat{\mathsf{Q}}(s)\cdot\hat{\mathbf{n}}(s), \tag{18}$$

where

$$\hat{\mathsf{Q}}(s)=s\hat{\mathsf{P}}(s)\cdot[\mathsf{I}-\hat{\mathsf{P}}(s)]^{-1}. \tag{19}$$

By inverse Laplace transformation of Eq. (18), we obtain a *non-Markovian equation of evolution* for the distribution vector:

$$\partial_t \mathbf{n}(t) = -(\mathsf{I}-\mathsf{F})\cdot\int_0^t d\tau\ \mathsf{Q}(\tau)\cdot\mathbf{n}(t-\tau), \tag{20}$$

which is to be solved with the initial condition $\mathbf{n}(0)=\mathbf{n}^0$. These equations are quite generally valid, for an arbitrary CTRW, with an arbitrary number of basins.

IV. IMPLEMENTATION OF THE CTRW MODEL

We now specialize the results for our simple three-basin case. The CTRW model of the standard map dynamics is defined by the *transition probability matrix* F and by the *waiting time distribution matrix* $\mathsf{P}(t)$. These quantities are determined from an analysis of several ''long'' chaotic orbits generated by the standard map. In the present work we used four such orbits, for $K=0.7$, each obtained by a total of N iterations from some initial condition. Their (arbitrary) labels and their characteristics are as follows:

$$\begin{aligned}
&\text{orbit } A: \quad x_0=0.25,\ \ \theta_0=0.00,\ \ N=25\,000,\\
&\text{orbit } B: \quad x_0=0.00,\ \ \theta_0=0.48,\ \ N=25\,000,\\
&\text{orbit } C: \quad x_0=0.12,\ \ \theta_0=0.40,\ \ N=24\,000,\\
&\text{orbit } D: \quad x_0=0.20,\ \ \theta_0=0.88,\ \ N=24\,000.
\end{aligned} \tag{21}$$

A time series was generated for each orbit and analyzed as described below. The three basins are labeled by an index $m=(1,2,3)$, defined at the beginning of Sec. III.

A. Transition probabilities

For each orbit, every jump from a basin m to a basin n is recorded: the total number of such jumps is denoted by $N_{n\leftarrow m}$ (for instance, in the section of orbit D shown in Fig. 4, we find $N_{2\leftarrow 3}=3$, $N_{3\leftarrow 2}=2$, $N_{1\leftarrow 3}=1$, $N_{3\leftarrow 1}=1$). These numbers must be converted to transition frequencies or probabilities $f_{n\leftarrow m}$ (for clarity we use in the present section an arrow between the subscripts of f_{nm}). In order to define the transition probabilities $f_{n\leftarrow m}$, we note that a particle leaving basin m can only jump into one of the two other basins, hence

$$\sum_n f_{n\leftarrow m}=1. \tag{22}$$

Using this normalization condition, we define a first set of empirical transition probabilities as follows:

$$\begin{aligned}
&f'_{2\leftarrow 1}=\frac{N_{2\leftarrow 1}}{N_{2\leftarrow 1}+N_{3\leftarrow 1}}, \quad f'_{3\leftarrow 1}=1-f'_{2\leftarrow 1},\\
&f'_{1\leftarrow 2}=\frac{N_{1\leftarrow 2}}{N_{1\leftarrow 2}+N_{3\leftarrow 2}}, \quad f'_{3\leftarrow 2}=1-f'_{1\leftarrow 2},\\
&f'_{1\leftarrow 3}=\frac{N_{1\leftarrow 3}}{N_{1\leftarrow 3}+N_{2\leftarrow 3}}, \quad f'_{2\leftarrow 3}=1-f'_{1\leftarrow 3}.
\end{aligned} \tag{23}$$

These numbers are calculated for each of the four orbits: the values obtained in this way are slightly different for each orbit, because of the limited statistics (typically, one finds the following values for $f'_{2\leftarrow 1}$ for our four orbits: $20/36=0.555$, $16/30=0.533$, $17/40=0.425$, $11/25=0.440$). Next, we note that the exact transition probabilities must also satisfy the following independent normalization, expressing that the particles entering basin n can only originate from one of the two other basins:

$$\sum_m f_{n\leftarrow m}=1. \tag{24}$$

This condition allows us to define an alternative set of approximate transition probabilities (for each orbit):

$$\begin{aligned}
&f''_{2\leftarrow 1}=\frac{N_{2\leftarrow 1}}{N_{2\leftarrow 1}+N_{2\leftarrow 3}}, \quad f''_{2\leftarrow 3}=1-f''_{2\leftarrow 1},\\
&f''_{1\leftarrow 2}=\frac{N_{1\leftarrow 2}}{N_{1\leftarrow 2}+N_{1\leftarrow 3}}, \quad f''_{1\leftarrow 3}=1-f''_{1\leftarrow 2},\\
&f''_{3\leftarrow 1}=\frac{N_{3\leftarrow 1}}{N_{3\leftarrow 1}+N_{3\leftarrow 2}}, \quad f''_{3\leftarrow 2}=1-f''_{3\leftarrow 1}.
\end{aligned} \tag{25}$$

These numbers are also calculated for each of the four orbits. They will be slightly different from the corresponding f''s (e.g., we find $f''_{2\leftarrow 1}$ for our four orbits: $19/35=0.543$, $16/42=0.381$, $17/52=0.327$, $11/25=0.440$). We now take the average as follows: for each pair (n,m) we add together the four values of $f'_{n\leftarrow m}$ and the four values of $f''_{n\leftarrow m}$ and divide the result by eight. The result is a matrix $\hat{F}$ whose elements are shown here together with the standard deviations; we also show the sum of the rows and of the columns, in order to check Eqs. (22) and (24):

	$m=1$	2	3	$\Sigma_n \hat{f}_{n\leftarrow m}$
$n=1$	0	0.47 ± 0.07	0.44 ± 0.07	0.91
2	0.46 ± 0.06	0	0.57 ± 0.08	1.03
3	0.48 ± 0.07	0.56 ± 0.08	0	1.04
$\Sigma_m \hat{f}_{n\leftarrow m}$	0.94	1.03	1.01	

(26)

We note the following points. The two sum rules are pretty well satisfied in spite of the rather small statistics. We also note that the matrix is very nearly symmetric. Finally, taking into account the standard deviations, this ''empirical'' matrix is compatible with the simplest choice implying maximum symmetry:

$$f_{n\leftarrow m}=\frac{1}{2}, \quad \forall m,\ \forall n\neq m, \tag{27}$$

or, in expanded form

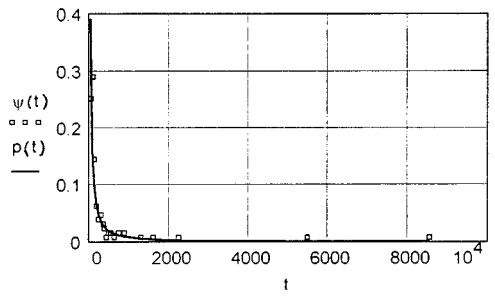

FIG. 5. Waiting time distribution for basin 1. Squares: measured values $\psi(t)$; solid curve: power law $p(t)$, given by Eqs. (30) and (31).

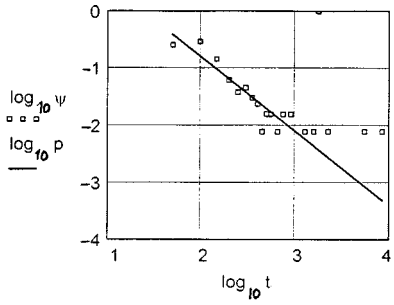

FIG. 6. Waiting time distribution for basin 1: same data as in Fig. 5, in a log-log representation.

$$\mathsf{F}=\begin{pmatrix} 0 & 0.5 & 0.5 \\ 0.5 & 0 & 0.5 \\ 0.5 & 0.5 & 0 \end{pmatrix}. \tag{28}$$

Given that the three basins are attached to a single island, this symmetry appears very reasonable.

B. The waiting time distribution

The successive times of sojourn in a given basin m, Δt_m, were measured sequentially in each of the four orbits available. For each basin m (and for each orbit) the number $N_m^{(q)}$ of occurrences in successive sectors of length 50 comprised between $t=q$ and $t=q+49$ was determined (e.g., the number of sojourns of length $0<\Delta t_3\leqslant 49$, in basin 3, then the number of sojourns of length $50\leqslant\Delta t_3\leqslant 99$, etc.): these numbers (for each m and each q) were summed for all orbits. Dividing these numbers by the total number of successive sojourns in basin m, a histogram is obtained, which is an estimate for the waiting time probability in basin m:

$$\hat{p}_m^{(q)}=\frac{N_m^{(q)}}{\Sigma_q N_m^{(q)}}. \tag{29}$$

(For the reader's information we note that the total number of sojourns in each of the three basins found for the four orbits analyzed here is $N_1^{\mathrm{tot}}=131$, $N_2^{\mathrm{tot}}=158$, $N_3^{\mathrm{tot}}=156$). The quantities $\hat{p}_m^{(q)}$ are plotted vs q, i.e., vs time.

As an example we show in Fig. 5 this plot for basin 1. It is clearly seen that the most frequent sojourns are relatively ''short,'' $\Delta t_1<1000$; there occur, however, rare sojourns of very great length, say $\Delta t_1=5500$ or 8500 (the latter represents about a third of a typical orbit considered here).

These data can be pretty well fitted with a power law distribution for a continuous time variable:

$$p_m(t)=A_m t^{-1-\alpha_m}. \tag{30}$$

The best values for the exponent α_m and for the constant A_m are determined by fitting a straight line to the points in a log-log plot (Fig. 6). [In fitting a straight line to the log-log plot we discarded the two or three points corresponding to the very long (but very rare) sojourns. These points show a strong positive deviation from the straight line (but they are not very deviant in the plot of Fig. 9). Actually this deviation is illusory: it is due to the factor $1/\Sigma_q N_m^{(q)}$ in the waiting time frequency (29). When additional orbits are considered, $\Sigma_q N_m^{(q)}$ increases rapidly, but the very long tail events remain very rare (of order 1): thus their frequency decreases strongly, and in a log-log plot the corresponding points are pushed down.]

We thus obtain the following values:

$$A_1=10^{0.5}, \quad \alpha_1=0.3\equiv\alpha,$$
$$A_2=10^{0.6}, \quad \alpha_2=0.5\equiv\beta,$$
$$A_3=10^{0.6}, \quad \alpha_3=0.5\equiv\beta. \tag{31}$$

V. EXPLICIT SOLUTION OF THE CTRW MODEL

We now return to the general solution of the standard map CTRW, Eq. (15), and apply it to our special three-basin case. The transition probability matrix F was determined in Eq. (28). The waiting time distributions are compatible with a power law defined by Eqs. (30) and (31). The former equation implies that the Laplace transforms of these functions are of the following asymptotic form for small s:

$$\hat{p}_m(s)=[1-B_m s^{\alpha_m}], \quad s\to 0. \tag{32}$$

Indeed, the inverse Laplace transforms of these functions are provided by a Tauberian theorem [17,19,27]:

$$p_m(t)=B_m\frac{\alpha_m}{\Gamma(1-\alpha_m)}t^{-1-\alpha_m}, \quad t\to\infty. \tag{33}$$

Thus, choosing

$$B_m=A_m\frac{\Gamma(1-\alpha_m)}{\alpha_m}, \tag{34}$$

combined with the values (31), we are in agreement with the empirically determined Eq. (30). Using Eqs. (16) and (17) together with Eqs. (28) and (32), expanding the result for small s, and performing the inverse Laplace transformation, we find after a lengthy but simple calculation the result, expressed as follows. We first introduce the provisional abbreviation:

$$C=\frac{B_2}{\Gamma(1-\beta)},$$

next, we define the functions $H_{ij}(t)$:

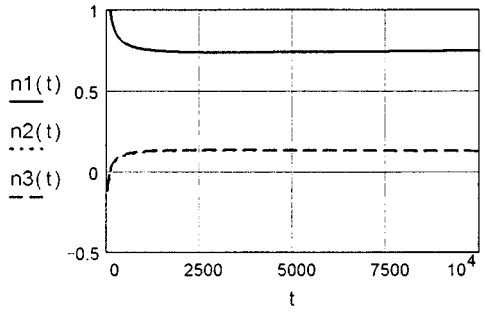

FIG. 7. Time evolution of probabilities of presence in basin m vs t. Solid, $n_1(t)$; dotted, $n_2(t)$; dashed, $n_3(t)$.

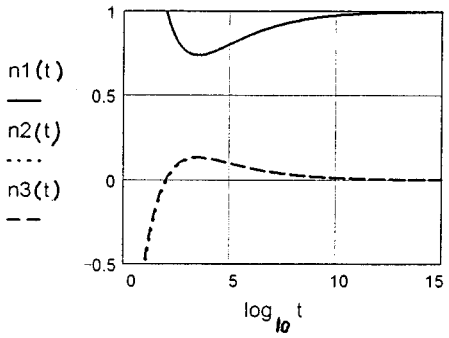

FIG. 8. Time evolution of probabilities of presence in basin m: same data as in Fig. 7, plotted vs $\log_{10} t$.

$$H_{11}(t)=1-\frac{2b}{\Gamma(1-\beta+\alpha)}t^{-(\beta-\alpha)}+\frac{4b^2}{\Gamma(1-2\beta+2\alpha)}t^{-2(\beta-\alpha)}+2\,Ct^{-\beta},$$

$$H_{12}(t)=H_{11}(t)-2\,Ct^{-\beta},$$

$$H_{21}(t)=\frac{b}{\Gamma(1-\beta+\alpha)}t^{-(\beta-\alpha)}-\frac{2b^2}{\Gamma(1-2\beta+2\alpha)}t^{-2(\beta-\alpha)}-Ct^{-\beta},$$

$$H_{22}(t)=H_{21}(t)+\frac{4}{3}Ct^{-\beta},$$

$$H_{23}(t)=H_{21}(t)+\frac{2}{3}Ct^{-\beta}, \tag{35}$$

where $b=B_2/B_1$. The asymptotic solution of the CTRW problem is then

$$n_1(t)=H_{11}(t)n_1^0+H_{12}(t)[n_2^0+n_3^0],$$

$$n_2(t)=H_{21}(t)n_1^0+H_{22}(t)n_2^0+H_{23}(t)n_3^0,$$

$$n_3(t)=H_{21}(t)n_1^0+H_{23}(t)n_2^0+H_{22}(t)n_3^0. \tag{36}$$

The following conservation law is easily checked:

$$n_1(t)+n_2(t)+n_3(t)=n_1^0+n_2^0+n_3^0. \tag{37}$$

The behavior of the solution is understood from Fig. 7. (In this and the following figures we take $n_1^0=0.5$, $n_2^0=0.05$, $n_3^0=0.45$.)

For very short times, we see a very rapid evolution; this region is, however, irrelevant. Indeed, in this range $n_1(t)>1$ and $n_2(t),n_3(t)<0$. The asymptotic regime expressed by Eqs. (36) begins to be valid, at least, for $t>200$, when all probabilities are in the physical domain. In the latter range, the evolution is *strikingly slow*. It is clear from Eqs. (35) and (36) that the final values of the probabilities are

$$n_1^\infty=1, \quad n_2^\infty=0, \quad n_3^\infty=0. \tag{38}$$

Note that this asymptotic solution results from the inequality $\alpha<\beta$. It is physically rather reasonable that after a long time all the particles end up in the basin corresponding to the entire island. As mentioned before, the evolution towards these values is very slow. The long time behavior is thus better seen on a semilog plot, showing $n_i(t)$ vs $\log_{10} t$ (Fig. 8).

Next, we note that the curves representing $n_2(t)$ and $n_3(t)$ are indistinguishable, in spite of our very unsymmetric initial condition. Indeed, as can be seen from Eqs. (35), the corresponding functions only differ by the terms proportional to $t^{-\beta}$, which are the most rapidly decaying ones. Thus, for sufficiently long times, the two curves coincide. Finally, by considering various values for n_i^0 it is found that the asymptotic evolution given by Eqs. (36) is remarkably insensitive to the initial conditions: after, say, $t=1000$, all curves are practically the same. On the other hand, as for any asymptotic approximation, the solution cannot be extrapolated back to $t=0$.

In order to determine the nature of the ''diffusion'' process, we now determine the evolution of the *mean square deviation* (MSD) as a function of time. It is naturally defined as follows:

$$\Sigma(t)=\sum_{j=1}^{3}\sigma_j^2 n_j(t), \tag{39}$$

where σ_j is the width of the basin j, which is determined graphically from the orbits plotted as in Figure 4. Indeed, during its sojourn in basin j, the particle oscillates with an amplitude of order σ_j. The following values are obtained:

$$\sigma_1=0.56, \quad \sigma_2=\sigma_3=0.26. \tag{40}$$

Given the slowness of the process, the function $\Sigma(t)$ is again plotted against $\log_{10} t$ in Fig. 9.

The initial descending section of the curve is irrelevant, because it lies in the unphysical range (i.e., the range where the probabilities lie outside the physical domain [0.1] and the asymptotic approximation is invalid). After the ''ghost minimum'' (which corresponds roughly to $t\approx 250$ for all initial conditions) the MSD increases very slowly towards an *asymptotic saturation value* Σ^∞, which is easily understood from Eqs. (38) and (39):

$$\Sigma^\infty=\sigma_1^2=0.314. \tag{41}$$

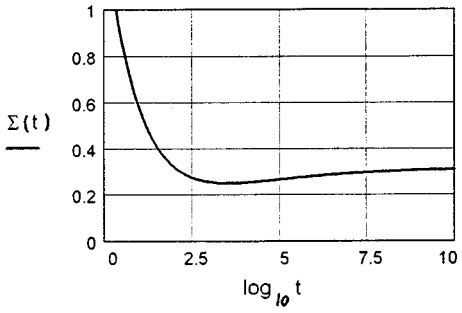

FIG. 9. Evolution of the mean square deviation, $\Sigma(t)$.

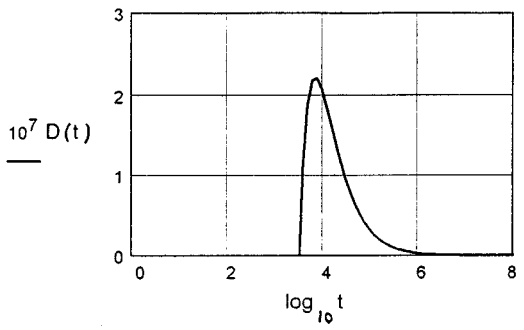

FIG. 10. The running diffusion coefficient $D(t)$.

We now consider the *running diffusion coefficient* $D(t)$, defined in the usual way:

$$D(t)=\frac{1}{2}\frac{d}{dt}\Sigma(t). \tag{42}$$

Its graph is given in Fig. 10 (plotted again vs $\log_{10} t$). Only the relevant (i.e., positive) part of the function is shown. The running diffusion coefficient is very small at all times ($\approx 10^{-7}$); after a maximum, it decays to zero as $t\to\infty$.

The asymptotic vanishing of the running diffusion coefficient and the corresponding saturation of the mean square displacement are the signature of a subdiffusive behavior of the standard map dynamics in the subcritical domain $K<K_c$*, i.e., in a regime of incomplete chaos.* This kind of behavior is not unexpected; the less obvious feature is the extreme slowness of the evolution. This shows that the stickiness of the islands is a very strong factor determining the slowing down of the evolution process.

One might think of investigating other diagnostics of chaotic motion for this strongly nondiffusive process. A possible candidate, which is very useful in a superdiffusive regime is the concept of *exit time* [28]. In the present case, however, this quantity is simply infinite, because the KAM surfaces bounding the region under consideration are strictly impermeable.

VI. CONCLUSIONS

In the present work we developed a way of simplifying the complex dynamics of an unstable system, such as the standard map. At the same time we derived a simple method for studying the ''strange diffusion'' appearing in this system in a subcritical regime. This feature is of interest in studies of anomalous diffusion of magnetic field lines in a toroidally confined plasma.

The feature responsible for the ''CTRW-like'' behavior of the standard map is the sticking of the orbits near the islands. As a result, the ''particles'' remain trapped for a possibly very long time in a single basin before jumping to another basin, where the scenario is repeated. This feature explains not only the overall subdiffusive nature of the motion (which is trivial, because of the presence of KAM barriers), but also the very slow evolution of the process. It may be recalled that the same sticking property produces superdiffusion when it appears near an island encircling an accelerator mode [12–15]. This type of behavior (which occurs in some windows of the supercritical domain, $K>K_c$) is not a generic property: accelerator modes are a specific feature of the standard map.

The simplification introduced in our model consists of retaining the interbasin transition probability and the waiting time distribution as the only random elements in the (chaotic) standard map motion. This is, of course, an oversimplification: the motion (of the x variable) inside a basin is not a perfectly regular oscillation; but this aspect will presumably not strongly affect the evolution of the MSD or the running diffusion coefficient.

This work is, of course, only a first step; many more aspects have to be studied. The calculations were developed in detail only for a simple three-basin situation. Our formulas (15)–(20) are, however, quite general and can be applied to a many-basin situation. A feature that is definitely lacking at present is an indication of the dependence of the phenomena on the stochasticity parameter K: this aspect will be an object of forthcoming work.

We also intend to study other maps by this method: this would serve a double purpose. First, it should show how generic the results are of the present study. Next, it should allow us to study more realistic models of tokamak or stellarator plasmas, in order to end up with a theory of strange and anomalous transport in such systems. This is our main, though remote, goal.

[1] M.F. Shlesinger, G.M. Zaslavsky, and J. Klafter, Nature **363**, 31 (1993).
[2] B. Chirikov, Phys. Rep. **52**, 265 (1979).
[3] A.J. Lichtenberg and M.A. Lieberman, *Regular and Stochastic Motion* (Springer, Berlin, 1983).
[4] E. Ott, *Chaos in Dynamical Systems* (Cambridge University Press, Cambridge, England, 1993).
[5] A.H. Boozer, Phys. Fluids, **27**, 2055 (1984).
[6] J.T. Mendonça, Phys. Fluids, B **3**, 87 (1991).
[7] H. Wobig, Z. Naturforsch. Teil A **42**, 1054 (1987).
[8] A.B. Rechester and R.B. White, Phys. Rev. Lett. **44**, 1586 (1980).
[9] A.B. Rechester, M.N. Rosenbluth, and R.B. White, Phys. Rev. A **23**, 2994 (1981).

[10] J.D. Meiss, J.R. Cary, C. Grebogi, J.D. Crawford, A.N. Kaufman, and H.D.I. Abarbanel, Physica D **6**, 375 (1983).
[11] H.H. Hasegawa and W.C. Saphir, in *Aspects of Nonlinear Dynamics*, edited by I. Antoniou and F. Lambert (Springer, Berlin, 1991).
[12] Y.H. Ichikawa, T. Kamimura, and T. Hatori, Physica D **29**, 247 (1987).
[13] T. Horita, H. Hata, R. Ishizaki, and H. Mori, Prog. Theor. Phys. **83**, 1065 (1990).
[14] R. Ishizaki, T. Horita, T. Kobayashi, and H. Mori, Prog. Theor. Phys. **85**, 1013 (1991).
[15] J. Klafter, M.F. Shlesinger, and G. Zumofen, Physics Today **49** (2), 33 (1996).
[16] E.W. Montroll and G.H. Weiss, J. Math. Phys. **6**, 167 (1965).
[17] E.W. Montroll and M.F. Shlesinger, in *Studies in Statistical Mechanics*, edited by J.L. Lebowitz and E.W. Montroll (North-Holland, Amsterdam, 1984), Vol. 11, p. 5.
[18] G.H. Weiss, *Aspects and Applications of the Random Walk* (North-Holland, Amsterdam, 1994).
[19] R. Balescu, Phys. Rev. E **51**, 4807 (1995).
[20] R.B. White, J.M. Rax, Y.L. Wu, M.N. Bussac, and L. Zuppiroli, in *Transport, Chaos and Plasma Physics*, edited by S. Benkadda, F. Doveil, and Y. Elskens (World Scientific, Singapore, 1994), p. 153.
[21] J.M. Greene, J. Math. Phys. **20**, 1183 (1979).
[22] R.S. McKay, J.D. Meiss, and I.C. Percival, Physica D **13**, 55 (1984).
[23] D.F. Escande, Phys. Rep. **121**, 165 (1985).
[24] J.D. Hanson, J.R. Cary, and J.D. Meiss, J. Stat. Phys. **39**, 327 (1985).
[25] J.D. Meiss and E. Ott, Phys. Rev. Lett. **55**, 2741 (1985).
[26] J.D. Meiss and E. Ott, Physica D **20**, 387 (1986).
[27] G. Doetsch, *Handbuch der Laplace Transformation* (Birkhäuser, Basel, 1955), Vol. II.
[28] S. Benkadda, Y. Elskens, and B. Ragot, Phys. Rev. Lett. **72**, 2859 (1994).